Archives of Biochemistry and Biophysics 505 (2011) 48–59

Contents lists available at ScienceDirect

Archives of Biochemistry and Biophysics

journal homepage: www.elsevier.com/locate/yabbi

PHK from phenol hydroxylase of *Pseudomonas* sp. OX1. Insight into the role of an accessory protein in bacterial multicomponent monooxygenases

Viviana Izzo [a,c,*], Gabriella Leo [b], Roberta Scognamiglio [a], Luca Troncone [a], Leila Birolo [b,c], Alberto Di Donato [a]

[a] Dipartimento di Biologia Strutturale e Funzionale, Università di Napoli Federico II, Via Cinthia, I-80126 Napoli, Italy
[b] Dipartimento di Chimica Organica e Biochimica, Università di Napoli Federico II, Via Cinthia, I-80126 Napoli, Italy
[c] School of Biotechnological Sciences, Università di Napoli Federico II, Napoli, Italy

ARTICLE INFO

Keywords:
Diiron
Hydroxylation
Metallochaperone
Monooxygenase
Phenol hydroxylase

ABSTRACT

Bacterial multicomponent monooxygenases (BMMs) are members of a wide family of diiron enzymes that use molecular oxygen to hydroxylate a variety of aromatic compounds. The presence of genes encoding for accessory proteins not involved in catalysis and whose role is still elusive, is a common feature of the gene clusters of several BMMs, including phenol hydroxylases and several soluble methane monooxygenases. In this study we have expressed, purified, and partially characterized the accessory component PHK of the phenol hydroxylase from *Pseudomonas* sp. OX1, a bacterium able to degrade several aromatic compounds. The phenol hydroxylase (ph) gene cluster was expressed in *Escherichia coli*/JM109 cells in the absence and in the presence of the phk gene. The presence of the phk gene lead to an increase in the hydroxylase activity of whole recombinant cells with phenol. PHK was assessed for its ability to interact with the active hydroxylase complex. Our results show that PHK is neither involved in the catalytic activity of the phenol hydroxylase complex nor required for the assembly of apo-hydroxylase. Our results suggest instead that this component may be responsible for enhancing iron incorporation into the active site of the apo-hydroxylase.

Introduction

Aromatic hydrocarbons released in the biosphere by human activities are today a major threat not only to the environment but also to human health due to their potential carcinogenicity [1]. By utilizing various catabolic pathways, microorganisms can use a wide array of aromatic compounds as the sole carbon and energy source, thus providing a set of diversified tools that can be used in bioremediation of contaminated environments [2,3]. In aerobic microorganisms, processing of aromatic compounds is initiated by oxygenases, in the so-called *upper pathway* [1,2]. These enzymes are responsible for the insertion of one or more oxygen atoms in the aromatic rings that, once activated, are further transformed by ring-cleavage dioxygenases that are part of a metabolic route called *lower pathway* [1,2]. The resulting products are then converted into metabolites of the tricarboxylic acid cycle (TCA), and eventually mineralized to carbon dioxide and water [1–4].

Bacterial multicomponent monooxygenases (BMMs)[1] are key enzymes of the upper pathway and catalyze the hydroxylation of the aromatic ring at different positions [4,5]. They usually consist of a 200–250 kDa hydroxylase component organized in a $(\alpha\beta\gamma)_2$ quaternary arrangement, a 10–16 kDa regulatory protein devoid of any cofactor and enhancing catalytic turnover, and a FAD- and (2Fe-2S) containing reductase that mediates electron transfer from NADH to the active site of the hydroxylase [4–6]. An additional Rieske protein may be present to assist the electron transfer between the reductase and hydroxylase components [4,7,8]. The hydroxylation chemistry takes place at a non-heme carboxylate-bridged diiron center coordinated by four glutamate and two histidine residues from a four-helix bundle [4–6,10]. Although the four-helix bundle motif and the diiron center are part of a conserved framework probably present in all BMMs [4,9], these enzymes differ considerably in subunit composition and dimension, arrangement of the coding sequences, and genomic localization which can be either chromosomic, or plasmidic [4,11].

* Corresponding author at: Dipartimento di Biologia Strutturale e Funzionale, Università di Napoli Federico II, Via Cinthia, I-80126 Napoli, Italy. Fax: +39 081 679313.
E-mail address: vizzo@unina.it (V. Izzo).

[1] *Abbreviations used:* BMM, bacterial multicomponent monooxygenase; ESI–MS, electro spray ionization mass spectrometry; ITC, isothermal titration calorimetry; LC-MSMS, liquid chromatography with tandem mass spectrometry detection; MALDI-TOF, matrix-assisted laser-desorption ionization-time of flight; MOPS, 3-(*N*-morpholino)propanesulfonic acid; PH, phenol hydroxylase; ORF, open reading frame; SDS–PAGE, sodium dodecyl sulfate polyacrylamide gel electrophoresis; sMMO, soluble methane monooxygenase; ToMO, toluene/*o*-xylene monooxygenase.

0003-9861/$ - see front matter © 2010 Elsevier Inc. All rights reserved.
doi:10.1016/j.abb.2010.09.023

Two different multicomponent monooxygenases, toluene *o*-xylene monooxygenase (ToMO) and phenol hydroxylase (PH) [12–20], have been identified in the genome of *Pseudomonas* sp. OX1, a bacterium able to grow on a wide spectrum of hydroxylated and non-hydroxylated aromatic compounds [12]. PH is a BMM composed of five polypeptides: PHL, PHM, PHN, PHO, PHP. These five polypeptide chains are organized as three components [20]. PHP is the NADH-oxidoreductase responsible for supplying electrons to the diiron cluster housed in the active site of the hydroxylase component. The hydroxylase comprises three polypeptides (L, N, O) organized in a quaternary structure of the type $(LNO)_2$. Finally, PHM has been shown to be a regulatory protein, devoid of any cofactor or metal, that is essential for efficient catalysis [20]. A comparative analysis of the polypeptide sequences of PH polypeptides showed a significant degree of identity with the components of the multicomponent phenol hydroxylase encoded by the *dmp* genes in *Pseudomonas* sp. CF600 [21–24], and with the constituents of toluene-*o*-monooxygenase (TOM) from *Burkholderia cepacia* G4 [25].

When the nucleotide sequence of the *ph* locus coding for the multicomponent phenol hydroxylase of *Pseudomonas* sp. OX1 was first determined, its 5′ region revealed the presence of a putative open reading frame (*orf*) whose deduced amino acid sequence shared 62.6% identity (74% similarity) to DmpK [21,26], a protein translated from an *orf* located at the 5′ of the gene cluster coding for the multicomponent phenol hydroxylase from *Pseudomonas* sp. CF600. DmpK has been shown not to be essential for *in vitro* phenol hydroxylase activity, but several lines of biochemical evidence suggested a major role for this protein in the expression of active recombinant hydroxylase [26].

DmpK is not a unique case among multicomponent monooxygenases. In fact, genes expressing a group of proteins usually indicated as *accessory* or *auxiliary proteins*, are frequently clustered together with the *orfs* coding for the other components of the BMMs [4,5]. These components share several common features: they are small proteins with a molecular mass of about 10 kDa, do not harbor any inorganic or organic cofactors, are expressed at low levels in their respective native organisms, and inhibit enzyme activity *in vitro* when present in stoichiometric amounts [27]. Despite these common aspects, the roles of the accessory proteins in BMMs have been elusive so far, although they have been hypothesized to be involved in the assembly of the active form of the hydroxylase component. This function is exemplified by biochemical studies of the protein MMOD, which was isolated from the methanotrophic bacterium *Methylococcus capsulatus* (Bath) and is part of the soluble methane monooxygenase (sMMO) system [6,27]. Despite a lack of sequence homology, similar genes encoding small proteins of unknown function have been identified across many different groups of BMMs [4,5,28–30], suggesting that the involvement of additional protein factors in the assembly of the active hydroxylase diiron centers might be more widespread than currently believed.

Accessory proteins recruited for the assembly of the metal cofactor in the active site are not a unique feature of BMMs, because proteins with similar roles have been described as common molecular tools to allow correct or efficient insertion of metals into the active sites of other metalloenzymes including Fe/S proteins, nitrogenase, urease and hydrogenase [26,31,32]. Different molecular mechanisms employed to facilitate the insertion of metal sites into target proteins have been reported in literature [32]. However, none of the mechanisms described so far have been unambiguously assigned to individual proteins such as DmpK and MMOD.

In this paper we describe a set of experiments aimed at gaining insight into the role of PHK, the accessory protein of phenol hydroxylase from *Pseudomonas* sp. OX1. The phenol hydroxylase gene cluster was cloned and expressed in *Escherichia coli* in the absence or presence of the *orf* coding for PHK. In the latter case, recombinant cells showed an increased phenol hydroxylase activity compared to cells not expressing PHK, suggesting a positive effect of the accessory protein on the enzymatic activity of phenol hydroxylase. Active $PH(LNO)_2$ and $PH(LNO)_2$/PHM complexes were purified from the soluble extract of cells expressing the complete *ph* gene cluster including *phk*. Additionally, we isolated a stable complex formed by PHK bound to a PH(LNO) trimer that was devoid of iron and hydroxylase activity and could not be reactivated under our experimental conditions. To elucidate the role of PHK, we subcloned and overexpressed this component in *E. coli* and characterized its interaction with the active hydroxylase moiety, $PH(LNO)_2$, showing that the protein is not directly involved in the catalytic activity of the phenol hydroxylase complex, as for MMOD and DmpK. However, PHK does not appear to be required for the production of active recombinant hydroxylase as observed previously for DmpK [26]. PHK seems instead to be involved in increasing the apparent affinity of apo-$PH(LNO)_2$ for iron, thus possibly facilitating the incorporation of the crucial transition metal into the active site of the protein.

Experimental procedures

Materials and general procedures

Bacterial cultures, plasmid purifications and transformations were performed according to Sambrook et al. [33]. The pET22b(+) expression vector and *E. coli*-strain JM109 were purchased from Novagen, whereas *E. coli*-strain BL21(DE3) was from Invitrogen. Platinum *Pfx* DNA polymerase used for PCR amplification was from Life Technologies. Enzymes and other reagents for DNA manipulation were from New England Biolabs. The oligonucleotides were synthesized at the MWG-Biotech (http://www.mwgdna.com). Q-Sepharose Fast Flow, Sephacryl S300 High Resolution, Sephadex G75 Superfine, Superdex columns and disposable PD10 desalting columns were from Pharmacia. All other chemicals were from Sigma. Ammonium hydrogen carbonate (AMBIC), Ethylenediaminetetraacetic acid (EDTA) and iodoacetamide were purchased from Fluka; Tri(hydroxymethyl)aminomethane (Tris), urea, dithiothreitol (DTT), and sequencing-grade trypsin were from Sigma. Formic acid and Acetonitrile (ACN) were purchased from Romil.

Expression and purification of recombinant PHM, PHP and C2,3O from *Pseudomonas* sp. OX1 are described elsewhere [20,34]. DNA fragments were sequenced at the MWG-Biotech (http://www.mwgdna.com).

Construction of expression vectors

The plasmid pGEM3Z/*phΔk* containing the *ph-lmnop orfs* was kindly supplied by Dr. Valeria Cafaro (Dipartimento di Biologia Strutturale e Funzionale, Università Federico II, Napoli, Italy). The plasmid pGEM7Z/*k* containing the *ph-klm orfs* was a gift of Dr. Carla Caruso (Dipartimento di Agrobiologia e Agrochimica, Università della Tuscia, Viterbo, Italy).

To allow the expression of the complete *ph* gene cluster, the DNA sequence encoding the PHK component was subcloned from plasmid pGEM7Z/*k* into vector pGEM3Z/*phΔk* to create a construct containing the *phk, phl, phm, phn*, *pho* and *php* genes. A DNA fragment comprising the entire *phk* gene and part of the *phl* genes was amplified from the pGEM7Z/*k* vector using standard PCR procedures. A *Sal*I restriction site was inserted at the 5′ end of the *phk* gene. The 3′ primer was designed to amplify an internal region of the gene *phl*, 180 nucleotides downstream of the ATG start codon, incorporating a *Mlu*I restriction site. The resulting recombinant plasmid, named pGEM3Z/*ph*, was verified by DNA sequencing. To

construct plasmid pGEM3Z/*phΔp*, pGEM3Z/*ph* was digested with the restriction endonuclease *Eco*RV which cuts the *php* gene at nucleotides 196 and 335 causing the deletion of a 140 bp fragment.

In order to overexpress PHK, a third construct was prepared that contained only the *phk* gene. The gene *phk* was first amplified using plasmid pGEM7Z/*k* as template and a PCR method that inserted *Nde*I and *BamH*I restriction sites at the 5′ and 3′ ends of the gene, respectively. The amplified fragment was digested with endonucleases *Nde*I and *BamH*I, ligated with the pET22b(+) vector previously cut with the same enzymes. The resulting recombinant plasmid, named pET/*phk* was verified by DNA sequencing and used to transform BL21(DE3) competent cells.

Expression of PHK and PH(LNO)$_2$

The gene products of plasmids pGEM3Z/*phΔk* and pGEM3Z/*phΔp* were expressed in *E. coli*-JM109 cells. PHK was expressed from pET/*phk* in *E. coli* BL21(DE3) cells. All recombinant strains were routinely grown in Luria–Bertani (LB) medium [33] supplemented with 100 μg mL^{-1} of ampicillin. Expression of recombinant proteins was induced by adding isopropyl-β-D-thiogalactopyranoside (IPTG) at a final concentration of 0.2 mM for pGEM3Z/*phΔk* and pGEM3Z/*phΔp*, and 0.1 mM for pET/*phk*. At the time of induction, $Fe(NH_4)_2(SO_4)_2{\cdot}6H_2O$ was added at a final concentration of 0.2 mM, except in the case of PHK from pET/*phk*. Growth was continued in all cases for 3 h at 37 °C. Cells were collected by centrifugation, washed in 25 mM of 3-(*N*-morpholino)propanesulfonic acid (MOPS), pH 7.0, containing 5% glycerol, and 2 mM L-cysteine (Buffer A). The cell paste was stored at −80 °C until needed.

Purification of the expression products of pGEM3Z/phΔp

The paste from a 2 L culture of induced cells was suspended in 40 mL of buffer A. Cells were disrupted by sonication (10 times for a 1-min cycle, on ice). Cell debris were removed by centrifugation at 18,000*g* for 60 min at 4 °C. The supernatant was immediately fractionated as described below. The soluble fraction from a 2 L culture of JM109 cells expressing the gene products of plasmid pGEM3Z/*phΔp* or pGEM3Z/*phΔk* was loaded onto a Q-Sepharose Fast Flow column (1 × 18 cm) equilibrated in buffer A containing 0.08 M NaCl at a flow rate of 10 mL h^{-1}. Elution was performed with a 500 mL linear salt gradient from 0.12 to 0.5 M NaCl in buffer A, at a flow rate of 18 mL h^{-1}. Fractions containing the proteins of interest were pooled, concentrated by ultrafiltration on an YM30 membrane, and loaded onto a Sephacryl S300 High Resolution column (2.5 × 50 cm) equilibrated in buffer A containing 0.2 M NaCl, at a flow rate of 8 mL h^{-1}. Fractions were pooled, concentrated by ultrafiltration on YM30 membranes, and stored under nitrogen at −80 °C. Unless otherwise stated, all chromatographic steps were performed at 4 °C. Buffers were purged by repeated cycles of flushing with nitrogen. Column operations were not strictly anoxic.

Purification of PHK

The soluble fraction from a 2 L culture of cells expressing the gene product of plasmid pET22b(+)/*phk* was loaded onto a Q-Sepharose Fast Flow column (1 × 18 cm) equilibrated in buffer A at a flow rate of 10 mL h^{-1}. Proteins were eluted with a 400 mL linear salt gradient from 0 to 0.45 M NaCl, at a flow rate of 10 mL h^{-1}. Relevant fractions were pooled, concentrated by ultrafiltration on YM10 membranes, and loaded onto a Sephadex G75 Superfine column (2.5 × 50 cm) equilibrated in buffer A containing 0.2 M NaCl at a flow rate of 8 mL h^{-1}. Fractions containing electrophoretically pure PHK were pooled, purged with N_2, concentrated by ultrafiltration on YM10 membranes, and stored at −80 °C.

Enzymatic assays

Enzymatic activities were measured as previously described [17] using phenol as a substrate and monitoring the production of catechol in a continuous coupled assay with recombinant catechol 2,3-dioxygenase from *Pseudomonas* sp. OX1 [34], which cleaves the catechol ring and produces 2-hydroxymuconic semialdehyde. Formation of this product, having an extinction coefficient of 12,000 M^{-1} cm^{-1}, can be monitored spectrophotometrically at 410 nm.

(i) *Assays of reconstituted PH components.* Conditions for this enzyme assay probing the activity of the reconstituted PH complex are reported elsewhere [17,20]. PH(LNO)$_2$ concentrations employed in the assay were typically 0.25–0.75 μM. Components PHP and PHM were added in a ratio of 2:4:1 compared to PH(LNO)$_2$ concentration. Semialdehyde yields were determined by measuring the absorbance at 410 nm. Specific activity (S.A.) was defined as nanomoles of substrate converted per minute per milligram (mU/mg) of PH(LNO)$_2$ hexamer at 25 °C.

(ii) *Whole-cells assays.* Whole-cells assays were performed as previously described [20] using *E. coli*-JM109 cells transformed with the plasmid of interest. One milliunit was defined as the amount of catalyst that oxidized 1 nmol of phenol per min at 25 °C.

(iii) *Assays on crude extracts.* Crude extracts of JM109 expressing either pGEM3Z/*ph* or pGEM3Z/*phΔk* were prepared by sonicating the cell suspension at an optical density at OD_{600} of about 7 in buffer A (3 times for a 1-min cycle, on ice). Cell debris was removed by centrifugation at 18,000*g* for 30 min at 4 °C. The supernatant was carefully decanted, and kept on ice. The reaction was carried out in 0.1 M Tris–HCl pH 7.5 in the presence of 0.25 mM NADH and 0.5 mM phenol. Semialdehyde yields were determined as noted.

Iron removal from PH(LNO)$_2$

Removal of iron from the hydroxylase component was performed as previously described [35] with the following modifications. A 1.2 mL solution of 10 μM PH(LNO)$_2$, 0.5 mM 1,10-phenanthroline in 0.05% HCl, and 0.8 mM methyl viologen in 25 mM MOPS (pH 7.0), was prepared in a glass vial fitted with a rubber septum and purged with nitrogen. A 20 μL aliquot of a 350 mM sodium dithionite solution, previously purged with a continuous flow of nitrogen, was added and the reaction mixture was incubated at room temperature for 3 h under a continuous flow of nitrogen. Apo-PH(LNO)$_2$ was separated from the reagents and from the $[Fe(o\text{-phen})_3]^{2+}$ complex by using a disposable PD10 desalting column (Pharmacia) equilibrated with a buffer containing 25 mM MOPS (pH 7.0), 200 mM NaCl, 5% glycerol and 2 mM L-cysteine (Buffer D). The mixture containing apo-PH(LNO)$_2$ (10 μM) was made anaerobic by purging the solution with nitrogen. Fractions of interest were pooled, concentrated and stored at −80 °C.

Isothermal titration calorimetry (ITC)

ITC experiments were performed on a Nano-ITC, CSC 5300 calorimeter from Calorimetry Science Corporation (Lindon, UT), having a cell volume of 1.3 mL. Calorimetric titrations were carried out at 25 °C, by injecting 10 μL aliquots of a 130 μM ligand solution into a 11 μM PHK solution at 200 s intervals for a total of 25 injections. The solution was stirred at 1000 rpm.

Analytical gel filtration

Analytical gel-filtration experiments were carried out as follows: 200 μL of a protein sample was loaded on a Superdex 200 HR 10/30 or on a Superdex 75 HR 10/30 column previously equilibrated in 25 mM Tris–HCl, 5% glycerol, 0.2 M NaCl and 2 mM L-cysteine, pH 7.0 installed on an AKTA™FPLC™ (GE Healthcare Life Science). The samples were eluted isocratically at room temperature at a flow rate of 0.5 mL min^{-1}. Protein separation was monitored at 280 nm. A molecular weight calibration was conducted in the same buffer with the following proteins of known molecular weight: apotransferrin (400 kDa), alcohol dehydrogenase (150 kDa), bovine serum albumin (66,000 Da), ovalbumin (45,000 Da), carbonic anhydrase (29,000 Da), trypsinogen (24,000 Da), cytochrome *c* (12,400 Da). When necessary, the area of each peak was estimated by nonlinear curve-fitting of the elution profile using PeakFit software (Systat Software).

Biotinylation of PHK

PHK (3.0 mg, in 25 mM MOPS pH 7.0, 5% glycerol, 0.2 M NaCl) was incubated with 1.37 mg of sulfosuccinimidobiotin (Sulfo-NHS-Biotin) (Pierce) dissolved in the same buffer at a molar ratio of 20:1, on ice in the dark for 2 h. The reaction was quenched with 0.1 M Tris–HCl pH 7.0 and the non-reacted biotin reagent was removed by size exclusion chromatography on a PD-10 column (GE-Healthcare) in 0.1 M Sodium Phosphate pH 7.2, 0.15 M NaCl. Absorbance at 220 and 280 nm was monitored to identify PHK-containing fractions. Appropriate fractions were pooled and added to Avidin Agarose Resin (settled gel, Pierce) in order to immobilize the biotinylated protein.

Immobilization of biotinylated PHK on avidin and "Pull down" assays

A 450 μL aliquot of resin was equilibrated with five volumes of Binding Buffer (0.1 M Sodium Phosphate pH 7.2, 0.15 M NaCl) and incubated with biotinylated PHK (3 mg biotinylated PHK per mL of settled avidin agarose resin) at 4 °C for 1 h. The resin was washed with 10 volumes of Binding Buffer.

Pseudomonas sp. OX1 cells grown on M9 minimal medium containing 5 mM phenol as a unique carbon and energy source were disrupted by sonication in 25 mM MOPS pH 7.0, 0.15 M NaCl, 5% glycerol, 1 mM PMSF containing a protease inhibitors cocktail (Sigma Aldrich). The extracts were centrifuged at 12,000 rpm for 1 h and filtered with a 0.45 μm polyvinylidene fluoride (PVDF) membrane. Total protein cell extracts, quantified using the BioRad protein assay, were incubated with 125 μl of mouse anti-IgG agarose conjugated beads (Sigma) overnight at 4 °C (preclining step). Cell extracts were then incubated with 450 μL of biotinylated-PHK immobilized on avidin resin and were incubated overnight at 4 °C. The resin was washed with 10 volumes of Binding Buffer and the protein samples were eluted with 70 μL of Laemmli sample buffer. Samples were analyzed by sodium dodecyl sulfate–polyacrylamide gel electrophoresis (SDS–PAGE) (12.5%, 20 cm × 20 cm), and proteins were stained with Coomassie Brilliant Blue G-Colloidal (Pierce, Rockford, USA).

Mass spectrometric analysis

Identification of complexed subunits was carried out on trypsin digested samples either by digestion in solution or *in situ* after separation by polyacrilamide gel electrophoresis. Proteins were detected on the gel using a colloidal Coomassie kit (Invitrogen Life Technologies). Excised bands were destained, reduced with 10 mM dithiothreitol (DTT), carbamidomethylated with 55 mM iodoacetamide in 0.1 M NH_4HCO_3 buffer, pH 7.5 and subjected to tryptic in-gel digestion for 16 h at 37 °C, by adding 100 ng of trypsin. Peak center fractions from analytical gel-filtration experiments (1 mL) were lyophilized, resuspended in 100 μl of H_2O, and digested at 37 °C for 16 h with 100 nmoles of trypsin. Reactions were quenched by lowering the pH to about 1 with formic acid, and the resulting peptide mixtures were concentrated and purified using a reverse phase Zip Tip pipette tips (Millipore). The peptides were eluted with 20 μL of a solution comprising 50% acetonitrile and 0.1% formic acid in deionized water. Peptide mixtures were analyzed either by matrix-assisted laser-desorption/ionization mass spectrometry (MALDI-MS) or capillary liquid chromatography with tandem mass spectrometry detection (LC-MSMS).

MALDI-MS experiments were performed on a Voyager DE-STR matrix-assisted laser-desorption ionization-time of flight (MALDI-TOF) mass spectrometer (Applied Biosystems, Framingham, MA) equipped with a nitrogen laser (337 nm). Typically, 1 μL of the total peptide mixture was mixed (1/1, v/v) with a 10 mg mL^{-1} solution of R-cyano-4-hydroxycinnamic acid in acetonitrile/50 mM citrate buffer (2/3, v/v). The experimental mass values obtained were compared with calculated masses from the predicted tryptic digestion of the different subunit sequences, confirming the identities of the corresponding protein bands.

The peptide mixtures were analyzed using a CHIP MS 6520 QTOF equipped with a capillary 1200 HPLC system and a chip cube (Agilent Technologies, Palo Alto, Ca). After loading, the peptide mixture (8 μl in 0.1% formic acid) was first concentrated and washed at 4 μL/min in a 40 nL enrichment column (Agilent Technologies chip), with 0.1% formic acid in 2% acetonitrile as the solvent. The sample was then fractionated on a C_{18} reverse-phase capillary column (75 μm × 43 mm in the Agilent Technologies chip) at flow rate of 400 nL/min with a linear gradient of eluent B (0.1% formic acid in 95% acetonitrile) in A (0.1% formic acid in 2% acetonitrile) from 7% to 60% over 50 min.

Peptide analysis was performed using data-dependent acquisition of one MS scan (mass range from 300 to 2000 m/z) followed by MS/MS scans of the three most abundant ions in each MS scan. Raw data from nanoLC-MSMS analyses were employed to query, using MASCOT software (Matrix Science, Boston, USA), a non-redundant protein databases (NCBI, with taxonomy restriction to Bacteria), or an *ad hoc* created databases including only the sequences of PHK, PHL, PHM, PHN, PHO.

Other methods

Polyacrylamide gel electrophoresis was carried out using standard techniques [33,36]. Tris–glycine gels (18% and 15%) were run under denaturing and native conditions respectively. SDS–PAGE "wide range" (200–6.5 kDa) molecular weight standard was from Sigma. Homology studies were performed by searching the public nucleotide and protein databases with BLAST. Total iron content was determined colorimetrically by complexation with Ferrozine [37]. Protein concentrations were determined colorimetrically with the Bradford Reagent [38] from Sigma, using 1–10 μg of bovine serum albumin (BSA) as a standard.

Results

Activity assays of whole cells of E. coli-JM109 expressing recombinant phenol hydroxylase in the presence or absence of PHK

To evaluate the influence of PHK on the phenol hydroxylase activity of PH, we initially investigated the catalytic activity of whole cells of *E. coli*-JM109 expressing the complete *ph l-m-n-o-p* gene cluster with or without *phk*, and compared the rate of conver-

sion of phenol to catechol by the induced cells in the presence or in the absence of the *phk* gene product.

To this purpose, the *orf* encoding PHK was amplified from plasmid pGEM7Z/*k* and subcloned into plasmid pGEM3Z/*phΔk* (see Construction of expression vectors). The primers used in the PCR reaction were designed to incorporate the putative PHK ribosome binding site (*rbs)* at the 5′ of the *phk* gene. This *rbs* was previously located at 8–10 bp upstream of the ATG start codon in the native 5′ UTR region of the *ph* gene cluster.

SDS–PAGE analysis of the crude extracts of induced cells expressing either pGEM3Z/*phΔk* or pGEM3Z/*ph* revealed that the hydroxylase components PHL, PHN and PHO were expressed at high levels from both plasmids. Additionally, no significant difference in the expression levels of PHM and PHP was observed. However, whole cells expressing the plasmid pGEM3Z/*ph*, showed a 2- to 4-fold increase in the rate of catechol production when compared to those lacking the expression product of gene *phk*. The latter had a specific activity of 0.8 ± 0.1 mU/OD_{600}; in the presence of gene *phk* the value of the activity with phenol was of 3.1 ± 0.5 mU/OD_{600}.

Similar results were obtained when crude extracts of *E. coli*-JM109 expressing either pGEM3Z/*ph* or pGEM3Z/*phΔk* were analyzed for catechol production. Recombinant *E. coli* cells harboring either plasmid were induced with 0.2 mM IPTG at 37 °C for 90 min and were collected by centrifugation. Crude extracts were prepared and used in continuous coupled assays as described in Enzymatic assays. A ~2–3-fold higher phenol hydroxylase activity was observed for crude extracts of *E. coli* expressing the *ph* gene cluster including gene *phk* than for those expressing the *ph* gene cluster in the absence of *phk*. Surprisingly, the activity of crude extract of *E. coli*-JM109 expressing pGEM3Z/*phΔk* could be restored to pGEM3Z/*ph* levels by adding 5 μM of exogenous iron (II). These results contrast those previously described for recombinant DmpK, where the addition of exogenous iron (II) was not sufficient to restore the enzymatic activity of the hydroxylase component in the absence of the auxiliary protein [26]. The total iron contents of crude extracts of cells expressing either pGEM3Z/*ph* or pGEM3Z/*phΔk* is similar, with 3.7 ± 0.7 nmol Fe/mg total protein and 4.2 ± 0.8 nmol Fe/mg total protein respectively, suggesting that PHK might be involved in directing intracellular iron to the hydroxylase moiety rather than influencing total amount of iron in the cell.

Purification and characterization of the expression products of pGEM3Z/phΔp

The results obtained on whole cells and on cells extracts of induced *E. coli* cells, described in the previous section, suggested a positive influence of the accessory protein PHK on the enzymatic activity of the phenol hydroxylase complex.

To gain additional insight into the role of PHK, we decided to purify PHK and all the other components of the phenol hydroxylase system from cells of *E. coli* expressing plasmid pGEM3Z/*ph*.

First a derivative of plasmid pGEM3Z/*ph*, having a partial deletion of the *php* gene, was constructed (see Construction of expression vectors). This construct was generated to avoid accumulation of indigo in the cell culture [39], which is the result of the hydroxylation of cellular aromatics by the active phenol hydroxylase system during induction of transformed *E. coli* cells.

Fractionation of the crude extracts of JM109 cells expressing pGEM3Z/*phΔp* was performed as described in the "Experimental procedures" section. Three distinct peaks eluted from the first anionic exchange column and were collected separately. As shown in Fig. 1A, all three peaks contained the PHL, PHN and PHO polypeptides of the hydroxylase protein, when analyzed by SDS–gel [20]. In peak 1, an additional protein band, with the molecular weight expected

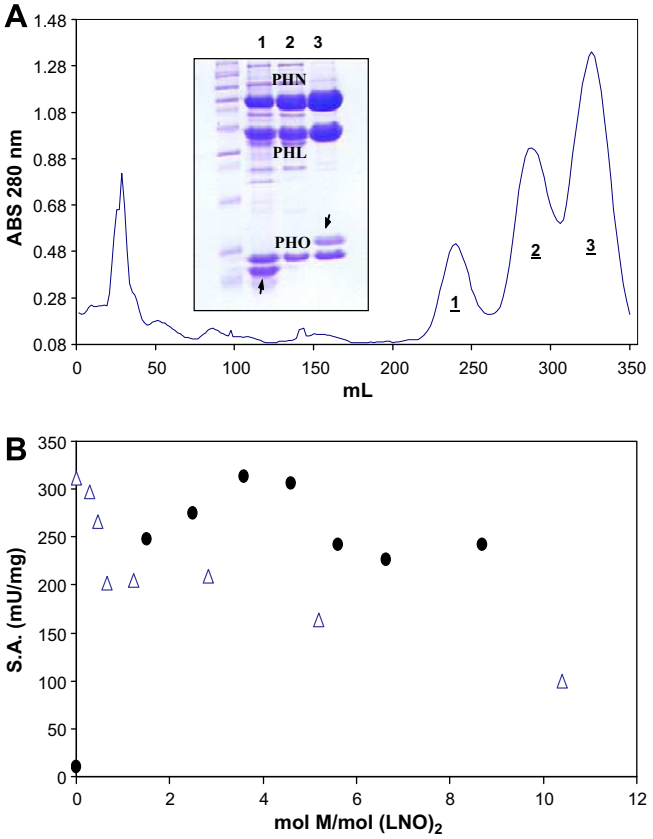

Fig. 1. Expression products of plasmid pGEM3Z/*phΔp*. (A) Q-Sepharose chromatogram and SDS–PAGE. MW, molecular weight standard ranging from 200 to 6.5 kDa (see Immobilization of biotinylated PHK on avidin and "Pull down" assays, for details). *Lane 1*, peak 1. *Lane 2*, peak 2. *Lane 3*, peak 3. Lane 2 contains the polypeptides PHN (60 kDa), PHL (38.3 kDa) and PHO (13.1 kDa). The arrows in lane 1 and 3 indicate the additional polypeptides, PHK and PHM respectively, that co-elute with the hydroxylase formed by subunits PHN, PHL and PHO. (B) Effect of different concentrations of regulatory protein PHM with respect to the hydroxylase $PH(LNO)_2$ on the rate of catechol production. The experiment was performed in the presence of either PHM–$PH(LNO)_2$ (empty triangles) complex isolated from peak 3, or $PH(LNO)_2$ (filled circles) isolated from peak 2. Optimized PHP/$PH(LNO)_2$ ratio of 4:1 was kept constant during the titration.

for PHK, was evident. In contrast the contents of peak 3 revealed a protein with the molecular weight expected for the regulatory protein PHM. The identities of the proteins of these three peaks were confirmed by peptide mass fingerprinting after *in situ* digestion of the bands excised from the gel and MALDI-TOF analyses.

Contents of the three peaks were further purified on a S-200 gel filtration column followed by anionic exchange chromatography on a Mono-Q column. Even after these purification steps, the composition and the ratio of the PH subunits of the three peaks remained as such, as evidenced by SDS–PAGE and mass spectrometry. These results strongly suggest the formation of stable complexes between the LNO subunits and PHK in peak 1, and between the LNO subunits and PHM in peak 3.

The protein complexes of all three peaks were individually characterized for iron content, molecular weight, and specific activity using phenol as a substrate. As shown in Table 1, the putative PHK-hydroxylase complex of peak 1 was devoid of both iron and enzymatic activity. The molecular weight of the putative complex measured by using a Superdex 200 gel filtration column accounted for a complex in which one molecule of PHK binds a trimeric LNO species. From now on we will refer to this complex as PHK-PH(LNO).

The same analyses carried out on peaks 2 and 3 (Table 1), revealed that peak 2 contains the hexameric hydroxylase with a qua-

Table 1

Pool	$Fe^{2+}/(LNO)_2$	Specific activity (mU/mg)	Calculated MW (kDa)	Expected MW (kDa)
1. PHK–PH(LNO)	ND[a]	ND[a]	136.30 ± 9.53	122.16
2. $PH(LNO)_2$	3.5 ± 0.2	254 ± 46	248.07 ± 2.31	223.58
3. PHM–$PH(LNO)_2$	4.2 ± 0.1	329 ± 17	259.30 ± 1.81	244.54

[a] ND, not detectable.

ternary structure of the type $PH(LNO)_2$, whereas peak 3 contains a complex in which two molecules of PHM binds the dimer $(LNO)_2$, from now on referred as PHM–$PH(LNO)_2$. The putative PHM–$PH(LNO)_2$ complex in peak 3 was fully active with phenol after the addition of an optimized ratio of the oxidoreductase component PHP (see Enzymatic assays and Fig. 1B). For peak 2, both the oxidoreductase and the recombinant component PHM, purified and characterized as described in Cafaro et al. [20], had to be added to obtain an optimally active catalytic system. In these latter experiments, 4 equiv. of PHM were added to $PH(LNO)_2$ for maximal activity (Fig. 1B). For both peak 2 and peak 3, adding higher concentrations of the regulatory component PHM inhibited the rate of phenol hydroxylation (Fig. 1B), [20].

Attempts to purify adequate amounts of PHK from cells expressing the whole *ph* gene cluster from pGEM3Z/*ph* were unsuccessful. Recombinant PHK was always found to be firmly bound to the trimeric complex PH(LNO) eluting in peak 1 and could not be dissociated unless strong denaturing conditions were used.

Purification and properties of PHK

To purify and characterize PHK, we subcloned the *orf* encoding this protein and expressed it in *E. coli*, strain BL21(DE3) (see Construction of expression vectors). Recombinant PHK was purified to homogeneity from *E. coli* harboring pET22b(+)/*phk* by an initial anionic exchange chromatography on a Q-Sepharose FF resin followed by a gel filtration step on a G-75 column (see Purification of PHK).

The oligomeric state of PHK was assessed by analytical gel filtration on a Superdex 75 analytical column. The chromatographic profile resulted in a single peak, which eluted at an apparent molecular weight of about 25,500 ± 400 Da, suggesting the occurrence of a dimeric species. The accurate subunit molecular weight of PHK was determined by electrospray ionization mass spectrometry (ESI–MS); the experimental value of 10,235.27 ± 0.19 Da is in agreement with the molecular weight predicted from the sequence of PHK (10,235.7 Da).

Purified PHK was found to be devoid of iron and did not contain any redox active prosthetic groups such as flavin, heme, or iron–sulfur centers. Incubation of PHK with an excess of ferrous iron and subsequent purification of the sample by using either a PD10 desalting column or dialysis did not lead the protein to retain any of the metal bound (data not shown).

Isothermal titration calorimetry (ITC) was then performed to assess whether PHK binds iron (II). 1 mL of purified 11 μM PHK in 25 mM MOPS pH 7.0 containing 5 mM L-ascorbic acid was titrated with the same buffer having 250 μL of 130 μM $Fe(NH_4)_2(SO_4)_2{\cdot}6H_2O$. L-ascorbic acid was added to both samples to avoid oxidation of iron (II) to iron (III) during the experiment. No binding isotherm was detected under the conditions reported in Materials and methods. To exclude the possibility that this result could arise from the oxidation of iron during the course of the experiment, the same experiment was repeated using a solution containing 130 μM $MnCl_2$ in 25 mM MOPS pH 7.0. Manganese (II) has already been used for replacing native iron (II) in several proteins ([35] and references therein). This metal is similar to iron (II) in charge and ionic radius and can exist in different oxidation states, but most notably its oxidation state (II) is much more stable at pH 7.0 when compared to iron (II). ITC experiments performed under conditions described above did not provide any evidence of binding between isolated PHK and manganese.

To provide evidence for the specificity of the binding event between PHK and the LNO subunits observed in the PHK-PH(LNO) complex isolated after the purification of the expression products of pGEM3Z/*phΔp* (see Purification and characterization of the expression products of pGEM3Z/*phΔp* and Fig. 1A), we carried out an affinity purification strategy using an avidin pull-down assay with extracts of cells of *Pseudomonas* sp. OX1 grown on phenol as a unique carbon and energy source (Fig. 2). This approach required recombinant biotinylated PHK. We biotinylated 3 mg of PHK as described in Biotinylation of PHK, with Sulfo-NHS-Biotin (sulfosuccinimidobiotin). To confirm that PHK was efficiently biotinylated under the experimental conditions, an aliquot was analyzed by RP-HPLC/ES-MS, which show that PHK contained up to 3 biotins per molecule. Biotinylated PHK was immobilized on avidin beads that were subsequently incubated with total protein extracts from *Pseudomonas* sp. OX1 cells grown on phenol; these latter had been pre-cleaned on agarose beads to minimize non-specific binding on the cromatographic matrix during the pull-down procedure. After extensive washing, PHK-recruited protein interaction partners were eluted in Laemmli buffer, separated on SDS–PAGE, and stained with colloidal blue Coomassie (Fig. 2). Three major proteins with molecular weights of ~12, ~40 and ~60 kDa (Fig. 2; lane 2) were identified. These proteins ran similarly to purified PHO, PHL and PHN standards on the gel (Fig. 2, lane 3). The three protein bands were excised from the gel, reduced, alkylated and digested *in situ* with trypsin. The resulting peptide mixtures were analyzed by LC-MSMS and the identities of the proteins were confirmed as PHO, PHL and PHN by comparing the MS patterns to those contained within the bacteria subset of

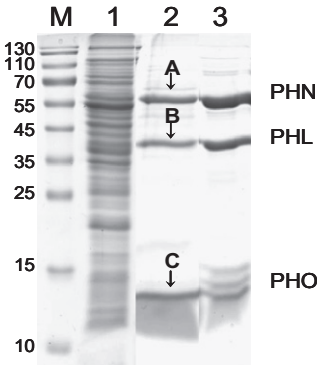

Fig. 2. Pull down experiment with biotinylated PHK. Colloidal blue-stained gel for biotinylated PHK associated proteins from *Pseudomonas* sp. OX1 cells grown on phenol (lane 2). Total *Pseudomonas* sp.OX1 cell extract is loaded in lane 1. An aliquot of PHM-$PH(LNO)_2$, was loaded (lane 3) as a control. Biotinylated PHK associated proteins were analyzed by SDS–PAGE followed by colloidal blue staining. A, B, and C labels in lane 3 indicate the three major proteins detected among the proteins pulled-down by biotinylated PHK.

the NCBI database using MASCOT software (Table S1, Supplementary Material). These results indicate a highly specific interaction of PHK with the LNO subunits of the hydroxylase moiety.

PHK-mediated inhibition of phenol hydroxylase activity

Once obtained the purified recombinant protein, the role of PHK was investigated by studying its influence on the phenol hydroxylase complex reconstituted from the purified components. Addition of purified PHK to the phenol hydroxylase complex reconstituted *in vitro* displayed a dose-dependent effect (Fig. 3). These assays contained PHP, PHM and $PH(LNO)_2$ at optimized ratios or PHP and the PHM–$PH(LNO)_2$ from peak 3 at optimized ratios with no exogenous recombinant PHM (see Enzymatic assays). Hydroxylation of phenol to catechol catalyzed by the *in vitro* reconstituted PH complex was measured at varying ratios of PHK to $PH(LNO)_2$. In all cases, addition of PHK resulted in the inhibition of the phenol hydroxylase activity (Fig. 3). Specifically, a 10-fold excess of PHK to $PH(LNO)_2$ resulted in only 16.8 ± 3.1% of the initial rate of catechol production. Interestingly, higher PHK:$PH(LNO)_2$ ratios did not lead to complete inactivation of phenol hydroxylase activity. A Kd value of 0.61 ± 0.15 μM over five different preparations of hydroxylase was obtained.

To gain further insight into the mechanism by which PHK inhibits its enzymatic activity, we incubated 57 μM of $PH(LNO)_2$ with 0.6 equiv. of purified PHK, in 500 μL of 25 mM MOPS pH 7.0. The mixture was let sit at room temperature for 90 min after which a 15 μL aliquot was analyzed on a native 15% polyacrilamide gel (Fig. 4A). Similar to a sample containing the partially purified PHK–$PH(LNO)_2$ complex from peak 1 (lane 1), the sample in which recombinant PHK was added to $PH(LNO)_2$ showed the presence of a high molecular weight species (lane 3) attributed to the trimeric form PH(LNO) associated to PHK (lane 1). Protein bands corresponding to the hydroxylase complex and uncomplexed PHK were also identified (lane 3) by comparison to a partially purified sample of $PH(LNO)_2$ (lane 2) and PHK (lane 4). The protein components of this putative identified PHK–PH(LNO) species were confirmed by peptide mass fingerprinting. The protein band from lane 3 was excised, digested *in situ* with trypsin, and analyzed by MALDI-TOF MS. Mass values were mapped onto the anticipated sequences of PHL, PHN, PHO, PHM, and PHK subunits confirming the presence of all four polypeptides (Table S2, Supplementary Material).

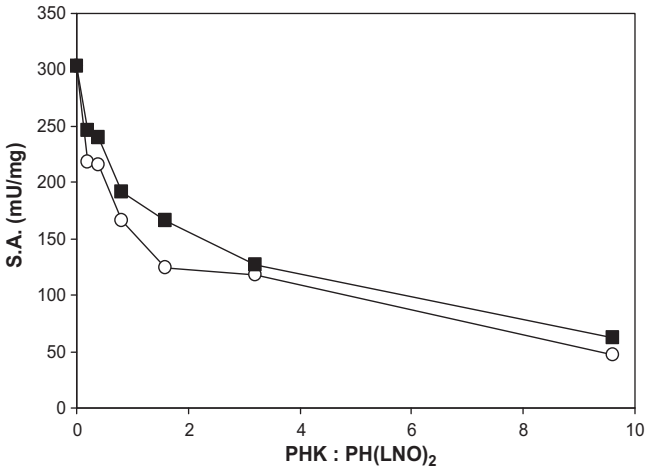

Fig. 3. Effect of increasing concentration of PHK on phenol hydroxylase activity of $PH(LNO)_2$. Activity assays were performed as described in Experimental Procedures. Filled squares represent experiments performed with the pre-formed PHM–$PH(LNO)_2$ complex. Empty circles are experiments with the $PH(LNO)_2$ complex employing exogenous recombinant PHM added at a 4:1 ratio with respect to the hydroxylase.

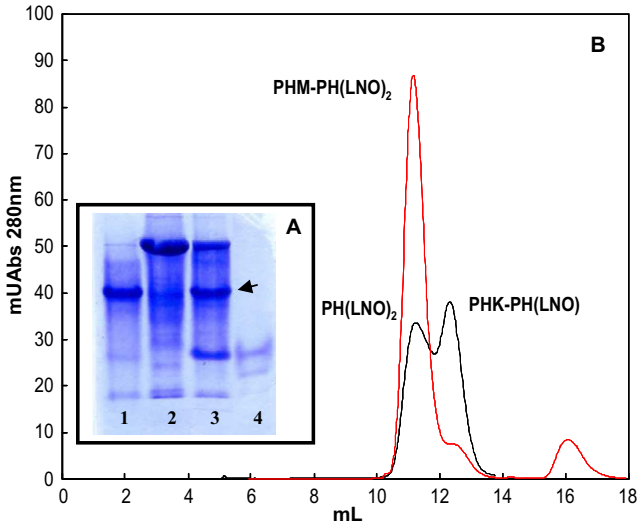

Fig. 4. Characterization of the $PH(LNO)_2$ complex in the presence of PHK. (A) Native gel electrophoresis of a $PH(LNO)_2$/PHK mixture. *Lane 1*, 10 μg of the PHK-PH(LNO) complex purified from peak 1 of the anion exchange chromatographic separation of Fig. 1. *Lane 2*, 20 μg of $PH(LNO)_2$ active hexamer. *Lane 3*, 20 μg of $PH(LNO)_2$ incubated with 0.6 equiv. of PHK for 90 min at room temperature. *Lane 4*, approximately 5 μg of purified recombinant PHK. The arrow indicates the additional band present in the incubated sample that is absent in the starting protein samples. (B) Elution profiles from analytical gel filtration chromatographic separation of a 200 μL mixture of 4.4 μM of $PH(LNO)_2$ and 2.2 μM of PHK (black line), and of a 200 μL mixture of 2.2 μM of PHM–$PH(LNO)_2$ and 4.4 μM of PHK (red line). (For interpretation of the references to color in this figure legend, the reader is referred to the web version of this article.)

The contents of the reaction mixture containing both $PH(LNO)_2$ and PHK were also analyzed by analytical gel filtration chromatography. A 200 μL aliquot of the mixture was run onto a Superdex 200 column. The elution profile (Fig. 4B) revealed a protein peak with an apparent molecular weight of 220 kDa, corresponding to the $PH(LNO)_2$ hexameric complex of the active hydroxylase, as assessed by running an authentic standard of $PH(LNO)_2$. Also evident is a species with an apparent molecular weight of 124 kDa, likely corresponding to the trimeric PH(LNO) species complexed with PHK. Fractions located in the peak centers were analyzed by SDS–PAGE and mass spectrometry (data not shown), confirming the presence of PHK only in the peak eluting with the apparent molecular weight of 124 kDa, whereas PHL, PHN, and PHO were observed in both peaks.

The molecular species produced by the interaction of PHK with the hexameric hydroxylase $PH(LNO)_2$ can be confidently assigned as a PHK-PH(LNO) complex. The observation that this species is devoid of both iron and catalytic activity with phenol, suggests that the inhibition of the phenol hydroxylase activity, demonstrated in *in vitro* assays and previously reported in the case of accessory proteins DmpK and MMOD [26,27], depends on the formation of apo-trimers of the type PH(LNO) and is mediated by the intervention of PHK.

Interestingly, incubation of PHK with the PHM–$PH(LNO)_2$ complex (peak 3 in Fig. 1), performed under the same experimental conditions, resulted in very little dissociation of the hexameric hydroxylase (Fig. 4B).

The PHK-PH(LNO) complex, obtained either from fractionation of crude extract of *E. coli*/pGEM3ZΔ*p* (Fig. 1A) or from the incubation of purified component PHK with hexameric $PH(LNO)_2$ complex (Fig. 4), could not be reactivated by any of our experimental procedures. In one of these experiments a 1.2 mL solution

containing 10 μM of PHK–PH(LNO) complex and 0.8 mM methyl viologen in 25 mM MOPS pH 7.0, was prepared in a glass vial fitted with a rubber septum and purged with nitrogen. Next, 20 μL of a 350 mM solution of sodium dithionite in 25 mM MOPS pH 7.0, prepared as described in Iron removal from $PH(LNO)_2$, and 24 μL of a freshly prepared 5 mM solution of $Fe(NH_4)_2(SO_4)_2{\cdot}6H_2O$ in deionized water, were added. The reaction mixture was incubated at room temperature for 3 h under a continuous flow of nitrogen. Excess, unbound iron was removed by gel filtration on a PD10 desalting column (Pharmacia) equilibrated in 25 mM MOPS pH 7.0, having 200 mM NaCl, 5% glycerol and 2 mM L-cysteine. Enzymatic assays performed on fractions containing the purified PHK–PH(LNO) complex revealed that no catalytic activity could be recovered under these conditions (Fig. 5A). Moreover, colorimetric assays using ferrozine to detect iron (see Other methods) demonstrated that the metal was not present in the protein sample tested (Fig. 5B).

In contrast, addition of excess iron to iron-depleted $PH(LNO)_2$ or PHM-$PH(LNO)_2$ complexes resulted in the significant recovery of both enzymatic activity and iron content of the purified protein (Fig. 5). Recovery of the maximal specific activity was of 35.1 ± 3.5% for $PH(LNO)_2$ and 78.9 ± 2.5% for PHM–$PH(LNO)_2$. The reason for the different values for the $PH(LNO)_2$ and PHM–$PH(LNO)_2$ complexes can be explained by the fact that while the formation of apo-hydroxylase from the $PH(LNO)_2$ species resulted in the complete removal of iron from the sample, ~50% of the original iron was retained when the metal depletion procedure was conducted with PHM–$PH(LNO)_2$. Importantly, these results were not dependent of the ratio of PHK to $PH(LNO)_2$ employed in the iron reconstitution procedures.

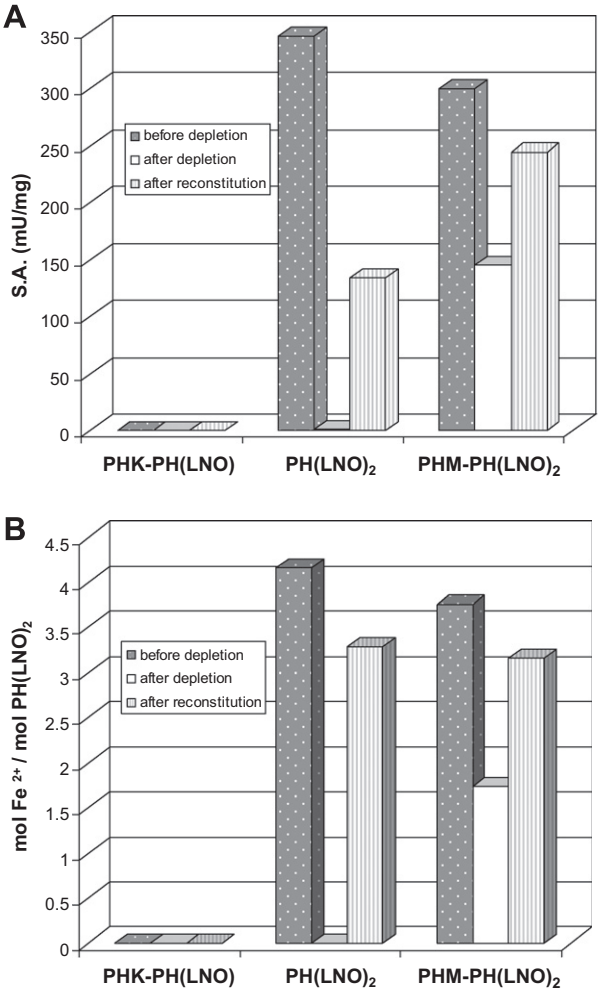

Fig. 5. Effect of iron depletion and reconstitution on the different purified hydroxylases expressed from plasmid pGEM3Z/*phΔp*. Iron content and phenol hydroxylase activity were measured as described in Materials and methods. Histogram A and B show the iron content and the residual phenol hydroxylase activities of the samples before and after depletion/reconstitution procedure, respectively.

Role of PHK in iron uptake of apo-PH(LNO)$_2$

Iron-depleted $PH(LNO)_2$, hereafter referred to as apo-$PH(LNO)_2$, was further purified by gel filtration on a S-200 gel filtration column. Two different species were obtained and identified by native-PAGE analysis and analytical gel filtration, which showed the presence of both hexameric apo-$PH(LNO)_2$ and trimeric apo-PH(LNO) complexes. Attempts to reconstitute the complexes with iron were performed by adding aliquots of a freshly prepared 50 μM solution of Fe(NH4)2(SO4)2·6H$_2$O in deionized water to 0.75 μM of either species in a 1 mL quartz cuvette. Immediately following iron addition, the other components of the phenol hydroxylase complex, the oxidoreductase PHP and the regulatory protein PHM, were added at a ratio of 2:1 and 4:1 with respect to $PH(LNO)_2$. Spectrophotometric continuous coupled assays were performed using phenol as substrate to monitor the rate of catechol formation.

Iron quantization of iron-reconstituted samples of apo-$PH(LNO)_2$ and apo-PH(LNO), in the absence or in the presence of PHK, always resulted in the measure of non-specific binding of iron to the hydroxylase. This is a common problem of *in vitro* iron reconstitution procedures. Since the enzymatic activity of the hydroxylase is related to the amount of iron correctly incorporated in the active site, we decided to indirectly measure iron binding by monitoring the increase in activity upon metal addition.

In the case of apo-PH(LNO) no enzymatic activity could be recovered after incubation with increasing concentration of iron (0–10 μM), neither in the presence of various amounts of recombinant PHK nor in its absence.

In the case of apo-$PH(LNO)_2$, different results were obtained in the absence and presence of PHK, which was added in a optimized ratio of 0.35:1 with respect to the iron-depleted hydroxylase protein (Fig. S1, Supplementary Material). As shown in Fig. 6, in the presence of PHK, addition of stoichiometric quantities of iron (II)

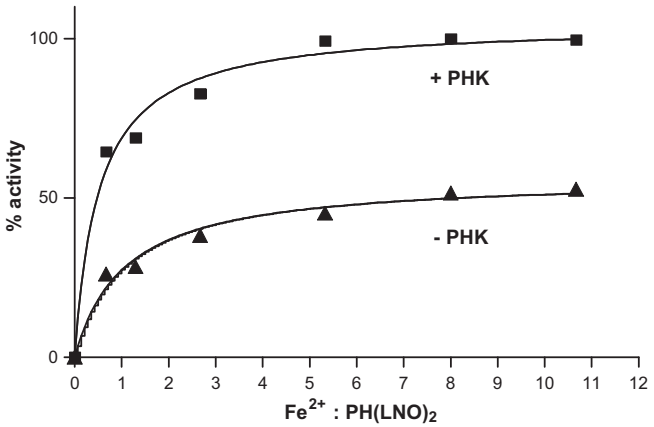

Fig. 6. Effect of increasing concentration of $Fe(NH_4)_2(SO_4)_2$ on the phenol hydroxylase activity of PH. Activity assays were performed as described in the Experimental procedures section in the presence (filled squares) or in the absence (filled triangles) of 0.35 equiv. of PHK with respect to apo-$PH(LNO)_2$. Values are normalized to the maximum specific activity obtained in the presence of accessory protein PHK.

to apo-PH(LNO)$_2$ resulted in the recovery of a maximal specific activity. Conversely, in the absence of PHK, only partial recovery (~50%) of apo-PH(LNO)$_2$ was possible when excess iron (II) was added to the reaction mixtures.

We cannot exclude the possibility that addition of a greater excess of iron (II) to apo-PH(LNO)$_2$ might allow for recovery of 100% of the activity obtained in the presence of PHK. Oxidation of iron (II) to iron (III) during the enzymatic assay hinders the use of high concentration of exogenous iron due to a background effect on the ABS410 monitored during the course of the reaction (see Enzymatic assays).

PHK-independent iron insertion into the hydroxylase at high iron (II) concentration was also demonstrated by the iron reconstitution experiments performed on whole cell extracts expressing either pGEM3Z/*ph* or pGEM3Z/*phΔk* and described in Activity assays of whole cells of *E. coli*-JM109 expressing recombinant phenol hydroxylase in the presence or absence of PHK. Using the same experiments performed on purified proteins and described in PHK-mediated inhibition of phenol hydroxylase activity (Fig. 5), apo-PH(LNO)$_2$ recovered specific activity with values comparable to those obtained in the presence or in the absence of accessory protein PHK when excess of exogenous iron (II) was added to the cell extracts. Together, these results suggest that PHK might facilitate iron uptake in the hexameric apo-PH(LNO)$_2$ complex, especially when the transition metal is present at low concentrations.

To evaluate the potential role of iron in the possible dissociation of the hexameric complex upon incubation with PHK, we monitored the distribution and subunit composition of the species obtained from gel-filtration experiments performed on iron-depleted samples incubated under different conditions (Fig. 7).

The identities of the subunits eluting in different peaks were assessed by a proteomic approach: 1 mL fractions taken from peak centers were digested with trypsin and analyzed by MALDI-TOF or, when ambiguous results were obtained, by capillary LC-MSMS. Proteins were then identified by comparing the experimental data to an in-house database using the MASCOT software. The protein sequences of PHL, PHN, PHO, PHK, and PHM were included in the search.

As observed with fully active holo-PH(LNO)$_2$, incubation of 2.5 μM of apo-PH(LNO)$_2$ with 1.25 μM of PHK at room temperature for 90 min, in a final volume of 200 μL, induced the dissociation of the hexameric species and facilitated the subsequent formation of PHK-PH(LNO) complexes, as measured gel-filtration experiments (Fig. 7, red line, and Table S3, Supplementary Material). Addition of either iron (10 μM) or exogenous regulatory protein PHM (10 μM) to the incubation mixture did not significantly alter the dissociation profile (data not shown).

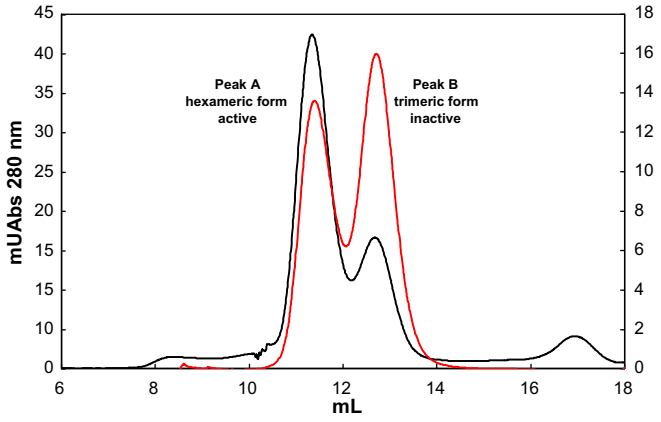

Fig. 7. Characterization of the apo-PH(LNO)$_2$ complex in the presence of PHK, PHM and iron. Elution profiles of an analytical gel filtration chromatographic separation of a 200 μL mixture of 2.5 μM of apo-PH(LNO)$_2$ and 1.25 μM of PHK (red line), and of a mixture of 2.5 μM of apo-PH(LNO)$_2$, 1.25 μM of PHK and 10 μM of PHM in the presence of 10 μM Fe^{2+} (black line). (For interpretation of the references to color in this figure legend, the reader is referred to the web version of this article.)

Importantly, a significant increase of the relative abundance of active hexameric species was observed with respect to the inactive trimeric form when exogenous recombinant PHM (10 μM) and iron (10 μM) were added simultaneously to the reaction mixture containing apo-PH(LNO)$_2$ and PHK (Fig. 7, black line). Moreover, in the later experiment a significant fraction of the regulatory protein PHM was bound to the active hexameric PH(LNO)$_2$ hydroxylase in a PHM-PH(LNO)$_2$ complex (Fig. 7, black line, and Table S3, Supplementary Material).

Unexpectedly, PHK did not bind to pre-formed, trimeric apo-PH(LNO). When apo-PH(LNO) was incubated with PHK, up to a molar ratio of 1:8, we could not detect any PHK co-eluting with the trimeric species. In these experiments the three hydroxylase subunits PHL, PHN, and PHO could be easily identified by proteomics methods (data not shown).

This result strongly suggests that PHK binds to the hexameric form (either apo- or holo-) of the hydroxylase before inducing dissociation to the PHK-PH(LNO) complex.

Discussion

Microorganisms devote part of their genetic and biochemical resources to ensure that cofactors are properly inserted into the active sites of metalloenzymes. Proteins responsible for the tightly regulated homeostasis of metals are generally known as metallochaperones [31,32]. These proteins also play a key role in preventing toxic metals – such as iron and copper – from engaging in non-specific interactions with cellular membranes, proteins, or DNA [32,40,41].

Based on biochemical studies of small BMM proteins similar to PHK from *Pseudomonas* sp. OX1, such as MMOD from *M. capsulatus* (Bath) and DmpK from *Pseudomonas* sp. CF600 [26,27], several roles could be envisaged for PHK. Possible functions include a molecular chaperone, a metal delivery factor, or a metallochaperone. Interestingly, sequences with high homology to that encoding PHK have been identified in most of the phenol hydroxylase operons sequenced so far [4,5], clearly suggesting a critical role for these components in this specific subfamily of BMMs.

We initially observed that *E. coli*-strain JM109 cells co-expressing recombinant multicomponent phenol hydroxylase from *Pseudomonas* sp. OX1 as well as the accessory subunit PHK were characterized by an improved catalytic ability to convert phenol to catechol when compared to the same strain expressing the PH operon devoid of the *phk* gene. This difference was confirmed when crude extracts of induced cells were used in the enzymatic assays instead of whole cells. Whereas total iron content was similar in cells expressing the two different *ph* gene clusters, a significant difference was observed in the ability of the cells to hydroxylate phenol. Surprisingly, cell extracts lacking recombinant PHK demonstrated an increase in hydroxylase activity when excess iron (II) was added. This result is different from what was previously observed with the recombinant hydroxylase of multicomponent PH from *Pseudomonas* sp. CF600 [26]. In this case the activity of crude extracts of cells not expressing the accessory component DmpK could be detected only after exogenous iron (II) and DmpK were both added, supporting the hypothesis that DmpK is involved not only in the delivery but also the proper insertion of iron into the active site of the hydroxylase [26].

The role of PHK was investigated here by initially studying its influence on the phenol hydroxylase complex reconstituted from the purified PHP (oxidoreductase), PHM (regulatory protein) and

$PH(LNO)_2$ (hydroxylase) components [20]. PHK was purified to homogeneity and found to be expressed as a dimer, devoid of any metal or organic cofactor. PHK was not essential for the enzymatic activity of the PH complex, when assayed with phenol, and instead inhibited the reaction even when present at low ratios with respect to the hydroxylase $PH(LNO)_2$ (Fig. 3).

An insight into the mechanism of phenol hydroxylase inhibition by PHK was obtained by characterizing the molecular species formed after incubating the hydroxylase complex $PH(LNO)_2$ with a sub-stoichiometric amount of purified PHK (Fig. 4). Native gel electrophoresis and gel-filtration experiments followed by mass spectrometric identification of the species formed upon incubation, showed that this is a novel molecular species comprised of PH(LNO) tightly associated with monomeric PHK. Biochemical assays revealed that this species is devoid of both iron and catalytic activity, providing an explanation for the inhibitory effect observed when exogenous PHK was added to reconstituted phenol hydroxylase in *in vitro* enzyme assays. The ability of PHK to promote dissociation of the hexameric complex $PH(LNO)_2$ was confirmed by the observation that inactive PHK–PH(LNO) could be isolated upon purification of cell extract of *E. coli*-strain JM109 expressing the complete *ph* gene cluster from plasmid pGEM3Z/*phΔp* (Fig. 1). In the same gel-filtration experiment the yield of the PHK–PH(LNO) complex was significantly lower when complex PHM–$PH(LNO)_2$ instead of $PH(LNO)_2$ was incubated with PHK (Fig. 4B). These results suggest a possible shielding effect of PHM towards the PHK-mediated dissociation of the $PH(LNO)_2$ hexamer, likely occurring in the absence of catalytic activity (Fig. 3).

Unexpectedly, experiments aimed at reactivating the PHK–PH(LNO) complex by the addition of exogenous iron (II) were not successful. Iron removal and restitution of $PH(LNO)_2$ and PHM-$PH(LNO)_2$ was possible when excess iron (II) was added, results that were somewhat independent of PHK (Fig. 5). Interestingly, iron removal from the hydroxylase was incomplete when PHM was present (Fig. 5). This "protective role" of the coupling protein PHM, observed in several experiments presented here, is similar to what previous reports of many BMMs described, as in the case of the sMMO system from *M. capsulatus* (Bath) [35].

Further insight on what appeared as contradictory results on the possible role of PHK came from attempts to incorporate iron into apo-$PH(LNO)_2$ hydroxylase. In the presence of the accessory protein PHK, complete recovery of the catalytic activity of apo-$PH(LNO)_2$ occurred when a stoichiometric concentration of iron (II) was added to the reaction mixture (Fig. 6). This observation is likely to be physiologically relevant. Notably, iron uptake and recovery of catalytic activity occurred at a much higher iron (II) concentration in the absence of PHK, a condition that is probably not compatible with the physiological concentration of this transition metal in the cell. This consideration also explains the observation that enzymatic activity was recovered when cell extracts of pGEM3Z/*phΔk* were incubated with iron (II), results that suggest the possibility that iron (II) can be inserted into apo-$PH(LNO)_2$ without the addition of exogenous PHK only when high concentrations of iron were present. In fact, many experiments probing PH were performed in the presence of an excess of $Fe(NH_4)_2(SO_4)_2$. Given the result presented here it is possible that these unnatural conditions might have prevented detection of the physiological role of PHK-like proteins in early experiments on BMMs. These experiments presented here show that at least in the PH from *Pseudomonas* sp. OX1, the accessory protein PHK is not necessary for proper diiron cluster assembly *in vitro*, a result that is different from what has been shown for the related component DmpK in *Pseudomonas* sp. CF600 [26].

Taking into account the data presented in this work and the information available in the literature for the accessory components MMOD [27] and DmpK [26], a possible mechanism (albeit incomplete) that does account for most of the observations and in which PHK might be involved can be hypothesized (Fig. 8).

Lacking experimental evidence on early post-translational events, the model assumes apo-$PH(LNO)_2$ as the starting point of the sequence of events. PHK transiently binds to the apo-hexamer, influencing the insertion of intracellular iron in the active site, and

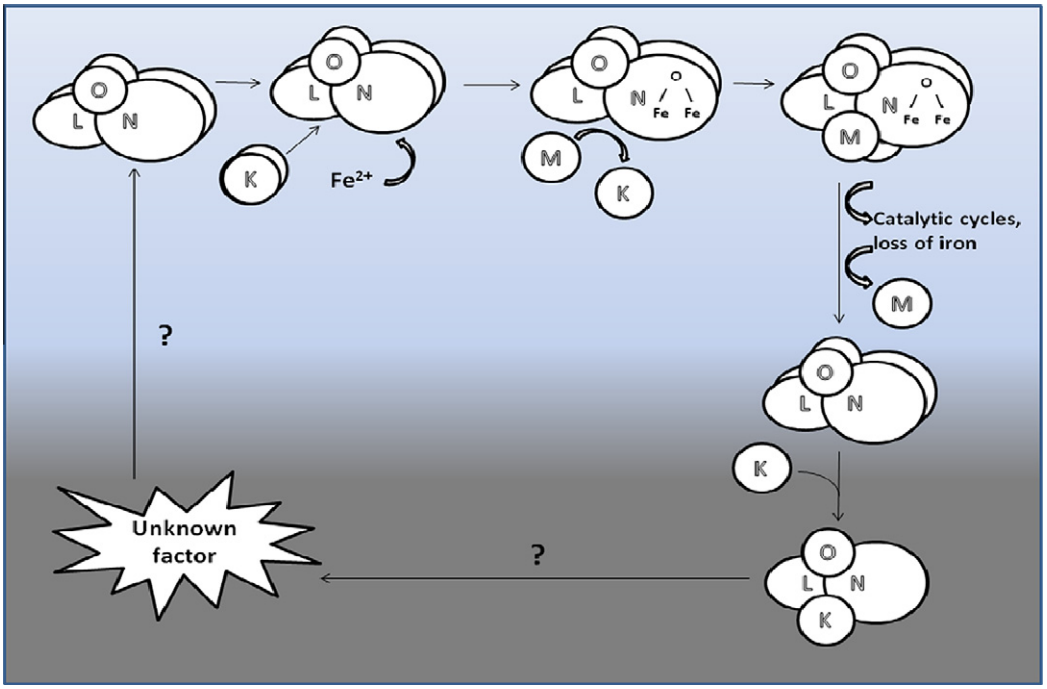

Fig. 8. Model showing a possible role for PHK. A possible model suggested by the experiments described in this paper and the data presented in literature for DmpK and MMOD accessory proteins [26,27]. In dark grey is the sequence of events that is still under investigation. The presence of the oxidoreductase PHP in the PH catalytic cycle has been omitted in the scheme for clarity.

thereby facilitating the formation of holo-PH(LNO)$_2$, the active hydroxylase complex.

Based on the ability of PHM to "protect" holo-PH(LNO)$_2$ from PHK-mediated dissociation (Fig. 4 and Fig. 7), our model proposes that the regulatory component PHM binds to the holo-PH(LNO)$_2$ complex immediately after the PHK-facilitated insertion of iron (II). This event displaces bound PHK, which can then be immediately recycled to assist in iron insertion in newly assembled apo-PH(LNO)$_2$ molecules.

In support of the existence of an interplay between the accessory and the regulatory proteins in BMMs, it should be underlined that Sazinsky and coworkers [35], using the purified components of the sMMO from *M. capsulatus* (Bath), highlighted, by means of ITC binding experiments, a preferential binding of the regulatory protein MMOB to the holo-hydroxylase complex MMOH and of the accessory protein MMOD to the apo-MMOH complex. Moreover, Powlowski and coworkers [26] had previously proposed that the accessory component DmpK likely interferes with the interaction between the regulatory protein DmpM and the hydroxylase moiety Dmp(LNO)$_2$.

Once the regulatory component PHM is bound to the PH(LNO)$_2$ active complex, the iron cofactor is protected within the active site from accidental loss, as indicated by our iron (II) removal and reconstitution experiments performed on the PHM–PH(LNO)$_2$ complex (Fig. 5). A new catalytic cycle can then be initiated (Fig. 8).

The protective role of the regulatory component in the phenol hydroxylase system of *Pseudomonas* sp. OX1 is particularly evident in the crystal structure of the PHM–PH(LNO)$_2$ complex [19]. This structure revealed that PHM blocks the entrance of solvent and substrate to the diiron active site, possibly offering protection of species formed at the dioxygen-activated metal center as it proceeds through its reaction cycle [19].

Our current hypothesis is that PHK does not directly bind iron, as suggested by ITC experiments, but instead might be responsible for altering the local conformation of apo-PH(LNO)$_2$, thus facilitating direct access of iron into the hydroxylase active site. We are currently investigating whether this observation is related to the direct binding of iron to an apo-PH(LNO)$_2$–PHK transitory complex or is a consequence of a conformational change induced by PHK in the iron-depleted hydroxylase moiety apo-PH(LNO)$_2$. The presence of iron in the active site of the PH(LNO)$_2$ hydroxylase could be made irreversible by rapid addition of O_2 once the two irons are in place, as already suggested in literature [42,43].

Among others, the question arises whether the PHK–PH(LNO) complex is of physiological importance. Our current hypothesis is that during repeated catalytic cycles the hydroxylase might lose iron which could induce the formation of the PHK–PH(LNO) species we observed *in vitro* (lower part of the scheme in Fig. 8). These complexes might reorganize, with the aid of further, yet undiscovered, auxiliary proteins, to form apo-PH(LNO)$_2$ species. Alternatively, the presence of PHK might be necessary to avoid the occurrence of holo-PH(LNO)$_2$ molecules *in vivo* in the absence of the regulatory protein PHM. In this case, the oxidoreductase PHP would still be able to transfer electrons to the hydroxylase moiety [20], leading to an uncoupling of NADH consumption and product formation, or a premature reduction of the oxygenated metal cluster, which would not only consume the reactive diiron species but also deplete the NADH supply of the cell in a wasteful manner [19].

At this stage we cannot exclude the possibility that formation of inactive PHK–PH(LNO) complexes could be just an artifact of our system due to the presence of high intracellular concentrations of recombinant PH(LNO)$_2$ and PHK. This phenomenon would shift the association equilibrium toward the formation of the PHK–PH(LNO) species. Nevertheless, the stable PHK–PH(LNO) complex might be a valuable tool to shed light on the molecular determinants responsible for the interaction between the accessory protein and the hydroxylase subunits PHL, PHN and PHO in future experiments.

In conclusion, novel details of the role of the accessory proteins in bacterial multicomponent monoooxygenases have been highlighted in the experiments presented here. These results add to what has been previously reported for accessory proteins MMOD and DmpK [26,27].

The similarities and differences between the different accessory proteins characterized to date lead to the conclusion that in the BMMs family seemingly similar protein components can have notably different ways of influencing the assembly of the diiron cluster in the active site of the hydroxylase moiety.

Acknowledgments

The authors are indebted to Prof. Giuseppe D'Alessio, Università di Napoli Federico II, for critically reading the manuscript, and to Dr. Luigi Martino and Prof. Tina Giancola, Università di Napoli Federico II, for ITC experiments.

This work was supported by a grant from the Ministry of University and Research (PRIN/2007).

Appendix A. Supplementary data

Supplementary data associated with this article can be found, in the online version, at doi:10.1016/j.abb.2010.09.023.

References

[1] S. Dagley, in: J. Sokatch, L.N. Ornston (Eds.), The Bacteria, vol. 10, Academic Press, Orlando, 1986, pp. 527–555.
[2] S. Harayama, K.N. Timmis, in: H. Sigel, A. Sigel (Eds.), Metal Ions in Biological Systems, vol. 28, Marcel Dekker, New York, 1992, pp. 99–156.
[3] E. Díaz, Int. Microbiol. 7 (2004) 173–180.
[4] E. Notomista, A. Lahm, J. Mol. Evol. 56 (2003) 435–445.
[5] J.G. Leahy, P.J. Batchelor, S.M. Morcomb, FEMS Microbiol. Rev. 27 (2003) 449–479.
[6] M. Merkx, D.A. Kopp, M.H. Sazinsky, J.L. Blazyk, J. Müller, S.J. Lippard, Angew. Chem. Int. Ed. 40 (2001) 2783–2807.
[7] J.D. Pikus, J.M. Studts, C. Achim, K.E. Kauffmann, E. Münck, R.J. Steffan, K. McClay, B.G. Fox, Biochemistry 35 (1996) 9106–9119.
[8] N.L. Elsen, L.A. Moe, L.A. McMartin, B.G. Fox, Biochemistry 46 (2007) 976–986.
[9] M.H. Sazinsky, S.J. Lippard, Acc. Chem. Res. 39 (2006) 558–566.
[10] L.J. Murray, S.J. Lippard, Acc. Chem. Res. 40 (2007) 466–474.
[11] H. Saeki, M. Akira, K. Furuhashi, B. Averhoff, G. Gottschalk, Microbiology 145 (1999) 1721–1730.
[12] G. Baggi, P. Barbieri, E. Galli, S. Tollari, Appl. Environ. Microbiol. 53 (1987) 2129–2132.
[13] G. Bertoni, F. Bolognese, E. Galli, P. Barbieri, Appl. Environ. Microbiol. 62 (1996) 3704–3711.
[14] G. Bertoni, M. Martino, E. Galli, P. Barbieri, Appl. Environ. Microbiol. 64 (1998) 3626–3632.
[15] P. Barbieri, F.L. Arenghi, G. Bertoni, F. Bolognese, E. Galli, Antonie Van Leeuwenhoek 79 (2001) 135–140.
[16] F.L. Arenghi, D. Berlanda, E. Galli, G. Sello, P. Barbieri, Appl. Environ. Microbiol. 67 (2001) 3304–3308.
[17] V. Cafaro, R. Scognamiglio, A. Viggiani, V. Izzo, I. Passaro, E. Notomista, Eur. J. Biochem. 269 (2002) 5689–5699.
[18] M.H. Sazinsky, J. Bard, J. Biol. Chem. 279 (2004) 30600–30610.
[19] M.H. Sazinsky, P.W. Dunten, M.S. McCormick, A. Di Donato, S.J. Lippard, Biochemistry 45 (2006) 15392–15404.
[20] V. Cafaro, V. Izzo, R. Scognamiglio, E. Notomista, P. Capasso, A. Casbarra, P. Pucci, Appl. Environ. Microbiol. 70 (2004) 2211–2219.
[21] I. Nordlund, J. Powlowski, V. Shingler, J. Bacteriol. 172 (1990) 6826–6833.
[22] J. Powlowski, V. Shingler, J. Bacteriol. 172 (1990) 6834–6840.
[23] J. Powlowski, V. Shingler, Biodegradation 5 (1994) 219–236.
[24] E. Cadieux, V. Vrajmasu, C. Achim, J. Powlowski, E. Münck, Biochemistry 41 (2002) 10680–10691.
[25] L.M. Newman, L.P. Wackett, Biochemistry 34 (1995) 14066–14076.
[26] J. Powlowski, J. Sealy, V. Shingler, E. Cadieux, J. Biol. Chem. 272 (1997) 945–951.
[27] M. Merkx, S.J. Lippard, J. Biol. Chem. 277 (2002) 5858–5865.
[28] D.L. Cardy, V. Laidler, G.P. Salmond, J.C. Murrell, Mol. Microbiol. 5 (1991) 335–342.
[29] H. Herrmann, C. Müller, I. Schmidt, J. Mahnke, L. Petruschka, K. Hahnke, Mol. Gen. Genet. 247 (1995) 240–246.
[30] P.M. Santos, I. Sá-Correia, J. Biotechnol. 131 (2007) 371–378.

[31] M.W. Ribbe, B.K. Burgess, Proc. Natl. Acad. Sci. USA 98 (2001) 5521–5525.
[32] J. Kuchar, R.P. Hausinger, Chem. Rev. 104 (2004) 509–525.
[33] J. Sambrook, E.F. Fritsch, T. Maniatis, Molecular Cloning: A Laboratory Manual, second ed., Cold Spring Harbor Laboratory Press, Cold Spring Harbor, New York, 1989.
[34] A. Viggiani, L. Siani, E. Notomista, L. Birolo, P. Pucci, J. Biol. Chem. 279 (2004) 48630–48639.
[35] M.H. Sazinsky, M. Merkx, E. Cadieux, S. Tang, S.J. Lippard, Biochemistry 43 (2004) 16263–16276.
[36] U. Laemmli, Nature 227 (1970) 680–685.
[37] C.J. Batie, E. LaHaie, D.P. Ballou, J. Biol. Chem. 262 (1987) 1510–1518.
[38] M.M. Bradford, Anal. Biochem. 72 (1976) 248–254.
[39] S. Hart, K.R. Koch, D.R. Woods, J. Gen. Microbiol. 138 (1992) 211–216.
[40] K.G. Daniel, R.H. Harbach, W.C. Guida, Q.P. Dou, Front. Biosci. 9 (2004) 2652–2662.
[41] T.B. Bartnikas, J.D. Gitlin, Nat. Struct. Biol. 8 (2001) 733–734.
[42] H.H. Nguyen, J. Ge, D.L. Perlstein, J. Stubbe, Proc. Natl. Acad. Sci. USA 96 (1999) 12339–12344.
[43] J. Ge, D.L. Perlstein, H.H. Nguyen, G. Bar, R.G. Griffin, J. Stubbe, Proc. Natl. Acad. Sci. USA 98 (2001) 10067–10072.